# Modulation of protein–protein interactions by synthetic receptors: Design of molecules that disrupt serine protease–proteinaceous inhibitor interaction

**Hyung Soon Park, Qing Lin, and Andrew D. Hamilton†**

Department of Chemistry, Yale University, New Haven, CT, 06520

Edited by Jack Halpern, University of Chicago, Chicago, IL, and approved February 8, 2002 (received for review December 17, 2001)

**In the present article we describe the design and evaluation of a synthetic receptor that binds to the exterior surface of chymotrypsin and disrupts its interaction with proteinaceous inhibitors, such as soybean trypsin inhibitor, basic pancreatic trypsin inhibitor, ovomucoid turkey inhibitor, and Bowman-Birk inhibitor. Using enzyme kinetics, nondenaturing gel electrophoresis, and gel filtration chromatography we show that the receptor is particularly effective at blocking the chymotrypsin-soybean trypsin inhibitor complex and that the mechanism involves formation of an initial ternary complex followed by a time-dependent displacement of the proteinaceous inhibitor.**

The design of synthetic molecules that can bind to a protein surface and block biologically important protein–protein interactions remains a major challenge (1). The principal difficulty lies in both matching the unsymmetrical distribution of polar and nonpolar domains on the protein as well as covering a sufficiently large surface area to achieve high affinity. In certain cases, particularly where well-defined clefts or cavities exist, some progress has been made in designing small molecules to bind to a protein surface. For example, guanidine esters have been designed to bind to IL-2 and block its interaction with its heterotrimeric receptor complex (2). Similarly, small heterocycles have been shown to bind to CD4 and disrupt its binding to MHC class II proteins on the surface of antigen-presenting T cells (3). Recently, several groups have shown that small molecules disrupt binding of the BH3 peptide of Bak to the Bcl-2/$Bcl_{XL}$ protein family with low micromolar $K_d$ values (4–6). Other approaches have used anionic polymers or oligomers such as aurintricarboxylic acid, heparin derivatives, and oligophenoxyacetic acid to target positively charged regions on a protein surface.

We have been interested in developing a potentially general strategy to protein surface recognition with the design of molecules that contain a large, functionalized, and variable interaction surface (7). Our approach borrows from the essential features of antibody-combining domains and is based on the attachment of several synthetic peptide loops onto a core calixarene scaffold. Interaction with a complementary protein surface can then involve significant contact (>400 Å$^2$) between the peptide loops and matching regions on the exterior of the protein (8). If binding occurs close to the active site or an area of contact with other proteins, then a disruption of the function of the protein can be anticipated. In this article we describe the application of this strategy to the disruption of the protein–protein complexes formed between the serine proteases and their proteinaceous inhibitors (PIs).

Peptide bond cleavage is an essential process in the activation or catabolism of numerous proteins. Proteolysis also plays important roles in such key cellular processes as signal transduction, metastasis, and apoptosis (9). However, the careful regulation of proteolysis is critical for the healthy function of the cell (10). Excessive proteolysis can lead to diseases such as emphysema, thrombosis, rheumatoid arthritis (caused by the uncontrolled complement cascade), and hyperfibrinolytic hemorrhage (10–12). Incomplete proteolysis can be similarly catastrophic as seen in Alzheimer's disease (13, 14), psorisis (15), tumor development (16), and infection by parasites and nematodes (17) (nematoic serpins protect the organism from proteolytic cleavage by host proteases).

A principal mechanism for controlling proteolysis involves secretion of highly selective PIs that bind to the surface of the protease and modulate its activity. Mammalian blood is a rich source of protease inhibitors, accounting for about 10% (by weight) of all plasma proteins in humans (18). The majority of complexes between proteases and their PIs are both stable and selective with a large surface area of contact between the two proteins (19). For example, Fig. 1 shows the crystal structures of four protease [chymotrypsin (ChT) or trypsin]–PI complexes that are the subject of this study: soybean trypsin inhibitor (STI), basic pancreatic trypsin inhibitor (BPTI), ovomucoid turkey inhibitor (OMTK), and Bowman–Birk inhibitor (BBI). In each case a loop from the PI projects into the ChT active site and a large area of protein surface on both ChT and the PI (1,350–1,600 Å$^2$) is buried on forming the complex.

The up- or down-regulation of PIs can result in a range of pathological conditions. For example, Alzheimer's disease, psoriasis, and certain tumors (caused by the inhibition of apoptosis) are thought to result in part from an up-regulation of specific protease inhibitors. One strategy for blocking the activity of up-regulated inhibitors would be to design synthetic agents that bind to the same region of the protease and prevent the association of the naturally occurring inhibitor. This goal brings into sharp focus the general difficulty of designing synthetic molecules to disrupt protein–protein interactions mediated over a large area (20). To our knowledge, there has been no example to date of a synthetic agent capable of blocking the interaction between a protease and its PI. In this article we describe the design and evaluation of a family of synthetic receptors that show potent protease-binding activity and are able to block interaction with specific PIs.

## Materials and Methods

**Materials.** ChT, BPTI, BBI, STI, and OMTK were all purchased from Sigma and used without further purification. Compound **1** was synthesized as described (21).

This paper was submitted directly (Track II) to the PNAS office.

Abbreviations: ChT, chymotrypsin; PI, proteinaceous inhibitor; STI, soybean trypsin inhibitor; BPTI, basic pancreatic trypsin inhibitor; OMTK, ovomucoid turkey inhibitor; BBI, Bowman–Birk inhibitor; BTNA, *N*-benzoyl tyrosine *p*-nitroanilide.

†To whom reprint requests should be addressed. E-mail: andrew.hamilton@yale.edu.

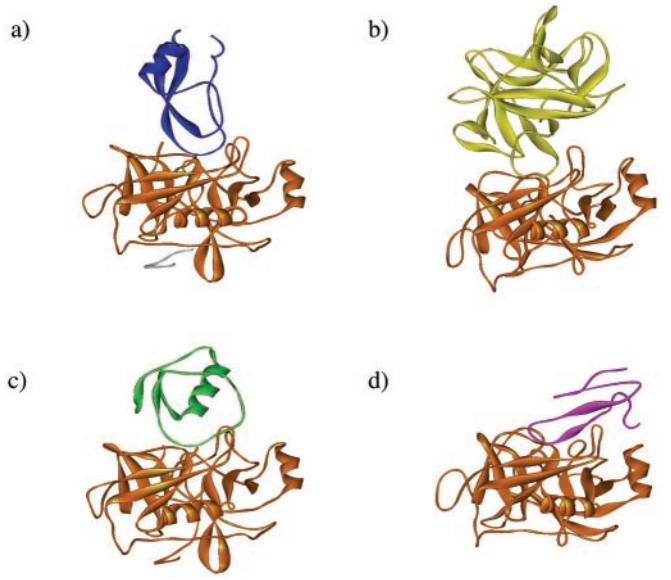


**Fig. 1.** Crystal structure of complexes between serine proteases and PIs. (*a*) ChT and BPTI (Protein Data Bank code 1CBW). (*b*) Trypsin and STI (Protein Data Bank code 1AVW). (*c*) ChT and OMTK third domain (Protein Data Bank code 1CHO). (*d*) Trypsin and BBI (Protein Data Bank code 1TAB). ChT and trypsin were fixed with orange color in the complexes.

**Enzyme Kinetics.** Hydrolysis of the chromogenic substrate *N*-benzoyl tyrosine *p*-nitroanilide (BTNA) by ChT was monitored over time at 410 nm with a UV plate reader (Molecular Devices). The enzyme reaction was initiated by adding BTNA (final concentration of 0.14 mM) into the enzyme solution (370 nM) in PBS, pH 7.4, and the initial velocity was calculated by the least-squares method with data points for the initial ≈5–10 min. For the time-dependent inhibition kinetics, a mixture of ChT, protease inhibitors, and **1** were incubated at room temperature for a maximum of 24 h. At certain time points a portion was withdrawn from the incubated solution and enzyme activity was measured.

**Gel-Shift Assay.** Nondenatured gel-shift assay was performed on thin (10 mm), 1% agarose gel in 5 mM Na-phosphate gel buffer. Four or 5 $\mu$l of sample was loaded on the gel, and power (constant 100 V) was applied for 30 min. The gel was fixed briefly in acetone, washed with water, and dried. The gel was then stained quickly with Coomasie blue R250 and destained in 10% acetic acid solution.

**Gel Filtration.** Approximately 15 ml of Sephadex 75 in PBS buffer, pH 7.4 was added to a 30 × 1 cm column. Ten microliters of each sample was applied to the column, and 0.2-ml fractions were collected for analysis.

**Docking Analysis.** Analysis of possible binding areas for **1** on the surface of ChT was carried out by using the AUTODOCK program

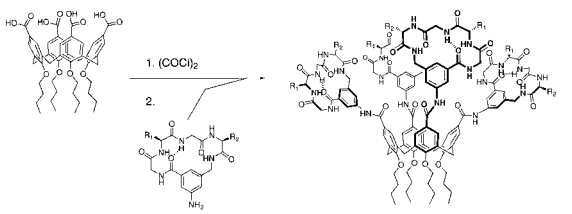


**Fig. 2.** Design and synthesis of protein binding agents.

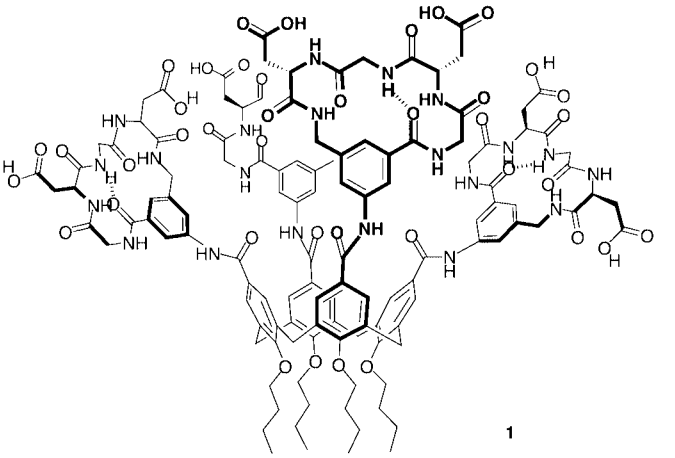

**Compound 1.**

(22–24). Because the number of atoms in **1** exceeds the number limit for running AUTODOCK, we removed the calixarene region of **1** from the coordinates and fixed the conformation of the remaining four peptide loops. After finishing the calculation, the whole molecule was reconstructed based on the coordinates obtained from the docking experiment. The coordinates of ChT were extracted from the coordinates of the ChT–BPTI complex in the Brookhaven Database (Protein Data Bank code 1CBW). With the exception of the construction of the coordinates, all other procedures were followed as outlined in the AUTODOCK manual for the docking experiment.

## Results and Discussion

The primary focus of our investigation was the enzyme ChT, which shows a strong preference for the cleavage of peptides with hydrophobic residues such as Tyr and Phe adjacent to the scissile peptide bond. Earlier we described an approach to the design of molecules that recognize a large area of the exterior surface of ChT and function as potent slow binding inhibitors to block the approach of small chromogenic substrates (21). This strategy involved the attachment of four synthetic peptide loops (each containing an amino-substituted 3-aminomethylbenzoic acid spacer) to a hydrophobic core scaffold based on a calix[4]arene unit (Fig. 2). By varying the sequence of the cyclic peptide a large number of functionalized surfaces with different recognition characteristics could be generated. The potential interacting surface area defined by these molecular scaffolds is 400–450 Å$^2$, permitting the targeting of a range of different proteins. In our earlier work we showed that compound **1**, containing a tetrabutoxy-substituted calix [4]arene linked to four loops with the Gly-Asp-Gly-Asp sequence, possessed submicromolar activity in blocking the approach of substrates into the active site of ChT. The eight carboxylate groups on **1** surround a core composed of the calix[4]arene and four aminomethylbenzoic acid units and create a highly anionic and hydrophobic surface. This region can be expected to interact favorably with cationic and hydrophobic domains on the surface of ChT. In particular a patch of several cationic groups is found near the active site cleft of the enzyme. In earlier studies (21) we have shown that **1** binds tightly to the cationic surface of ChT but does not interact with a corresponding anionic protein, such as the PI STI. To determine the optimal area on ChT to which **1** binds, a computational docking experiment using the AUTODOCK program was carried out. These simplified docking calculations (see *Materials and Methods*) point to a complex of the type shown in Fig. 3 where the carboxylate groups in **1** make contact with several of the of basic residues (Lys-90, -170, -175, -177, and Arg-145) around the active

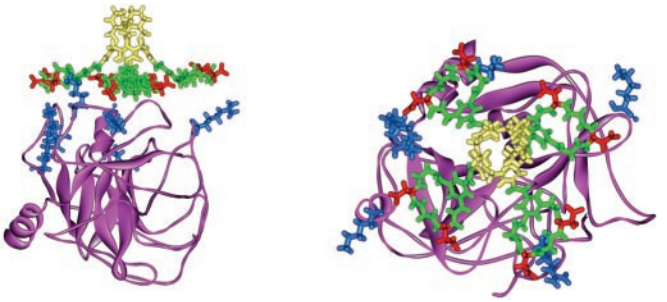

**Fig. 3.** Calculated structure (using AUTODOCK) for the interaction of **1** with ChT.

site cleft of ChT. A second possible binding area (not shown) was suggested by the docking experiments and centered on a hydrophobic patch including Val-60, -61, and -62. Compound **1**, presumably by binding to the surface of ChT close to the active site, showed competitive two-step slow binding inhibition behavior with $K_i$ and $K_i^*$ values of 0.81 and 0.11 $\mu$M, respectively (21). ChT is known to be inhibited by several proteins, including anti-ChT, STI, BPTI, OMTK, and BBI. Most of these PIs bind onto the same face of ChT containing the active site cleft (Fig. 1). We therefore wanted to test whether synthetic receptor **1** might also be able to disrupt the protein–protein interactions involved in stabilizing the ChT–PI complex.

**Time-Dependent Inhibition of ChT by Synthetic Receptor 1 in the Presence of Proteinaceous Inhibitors.** We first investigated the effect of **1** on the inhibitory activity of a series of PIs with respect to ChT. Complex formation between ChT and the different PIs results in a loss of hydrolytic activity against small substrates such as BTNA. The binding affinities of the four PIs used in this study are strong enough ($K_d$ values ranging from $10^{-7}$ to $10^{-12}$ M) for ChT activity to be inhibited by >90% in the 1:1 mixture at submicromolar (370 nM) concentrations. The effect of **1** varied depending on the different 1:1 ChT–PI complexes. In general, receptor **1** caused an initial recovery in ChT catalysis followed by a gradual loss of hydrolytic activity (Fig. 4). This result can be seen most clearly in the case of STI where the ChT–STI complex (Fig. 4, ●) shows less than 10% of the hydrolytic activity against BTNA compared with ChT alone (because of slow STI proteolysis this recovery increases to nearly 40% over time). However, addition of **1** (Fig. 4, ○) leads to an initial recovery of ChT activity to more than 50% of that of ChT before undergoing steady time-dependent inhibition. A similar, although smaller, effect is seen with the ChT–OMTK complex (Fig. 4, triangles), which initially recovers ≈30% enzyme activity on addition of **1** before undergoing time-dependent inhibition. In the case of ChT–BBI (Fig. 4, inverted triangles) both effects (recovery and later inhibition) are smaller, although reproducible. The one exception was the ChT–BPTI complex (Fig. 4, squares), which showed little effect on addition of **1**. This observation of initial recovery followed by inhibition suggested a two-step process in which **1** initially disrupts the inhibitory effect of the PI and then exerts its own inhibitory effect in a time-dependent manner. The initial recovery may be caused by a direct displacement by **1** of the PI from the surface of ChT or to formation of a ternary complex that induces a conformational change in the ChT–STI complex, allowing the approach of small substrates toward the active site (Fig. 5). We have previously shown that **1** is a strong and competitive time-dependent inhibitor of ChT. The gradual loss of activity in the second step presumably reflects formation of the aforementioned ChT–**1** complex.

A final feature of this experiment is that both STI and BBI show a steady loss of inhibitory activity with ChT over time. This loss is presumably caused by a slow proteolysis of the PI by ChT. In the presence of **1** no increase in proteolytic activity in the ChT–STI or ChT–BBI complex is observed with the level of inhibition after 1,500 min being larger than in the absence of **1**. The artificial receptor appears to confer a protection on the PI, removing it from proximity to the active site and its possible cleavage. No such loss of inhibitory activity is seen in the ChT–**1** complex. HPLC analysis of the reaction mixture at the end of the kinetics experiment shows no hydrolytic degradation in the structure of **1** (21).

The initial recovery of enzyme activity in the ChT–PI complexes (at 350 nM) was monitored as a function of changing the concentration of **1** (Fig. 6). In the case of STI, the activity of ChT was 80% that of the free enzyme at the end of the titration (14 $\mu$M). With BPTI there was little change whereas BBI and OMTK showed intermediate effects, recovering 30% activity at 14 $\mu$M. These results are consistent with an initial disruption of the ChT–PI complex by **1** leading to a restoration of access of the BTNA substrate to the active site.

**Gel Electrophoresis.** To investigate the mechanism by which **1** replaces the effects of the PI we carried out nondenaturing agarose electrophoresis on the different complexes. Mixtures of ChT, PI, and **1** were incubated for 10 min and 24 h and loaded onto the 1% agarose gel. The electrophoresis was completed within 20 min, and gels were stained by Coomasie blue R250. Comparison of gels 1 and 2 (Fig. 7) shows that a clear gel shift occurs on forming the ChT–PI complexes. Short-term incubations (10 min) of the complexes with **1** led to a further gel shift in all cases with no apparent dissociation of the PI from ChT, suggesting ternary complex formation. However, after 24 h incubation, the mixture of STI–ChT and **1** clearly shows a band for dissociated STI and one corresponding to the complex ChT–**1** (21). The other complexes (of ChT with BPTI, BBI, and OMTK) do not appear to change over a longer incubation period.

**Size-Exclusion Chromatography.** The displacement of STI by **1** was confirmed by size-exclusion chromatography. Sephadex G75 was packed into a 1-cm diameter column and equilibrated with 5 mM phosphate buffer, pH 7.4. The protein and receptor mixtures (10 $\mu$l of $2 \times 10^{-5}$ M) were loaded onto the column and eluted with a flow rate of 0.25 ml/min. Collected fractions were monitored by a UV-visual microplate reader at 280 nm, and the results are shown in Fig. 8. ChT alone gave a slow eluting band [around fraction number (FN) 50]. On addition of one equivalent of STI, a band with a shorter retention time (around FN 34) was observed, corresponding to the larger molecular weight species formed by complexation between ChT and STI. However, incubation of **1** (3.5 $\mu$M) with the ChT–STI complex for 10 min gave a band with an even shorter retention time (FN 28), suggesting the formation of a larger, ternary complex. Extending the incubation period to 36 h leads to a dramatic change in the size-exclusion chromatogram. In place of the fast moving band is seen a slow moving and broad band (around FN 46) corresponding to a species with a molecular weight slightly higher than ChT itself (molecular weight 24,700), presumably the ChT–**1** complex (molecular weight 27,400). The broadness of the band is also consistent with overlapping elution of the ChT–**1** complex and the displaced, but similarly sized, STI (molecular weight 20,000).

In this article we have shown that a synthetic molecule with a large and functionalized surface area is able to disrupt the interaction between ChT and certain members of the family of PIs. A comparison of the structures of the four ChT–PI complexes used in this study shows interfacial surfaces of 1,600, 1,390, 1,500, and 1,460 Å$^2$ for STI, BBI, OMTK, and BPTI, respectively. Despite its large interfacial surface, the ChT–STI complex has the weakest affinity with a $K_d$ value of $1.0 \times 10^{-7}$

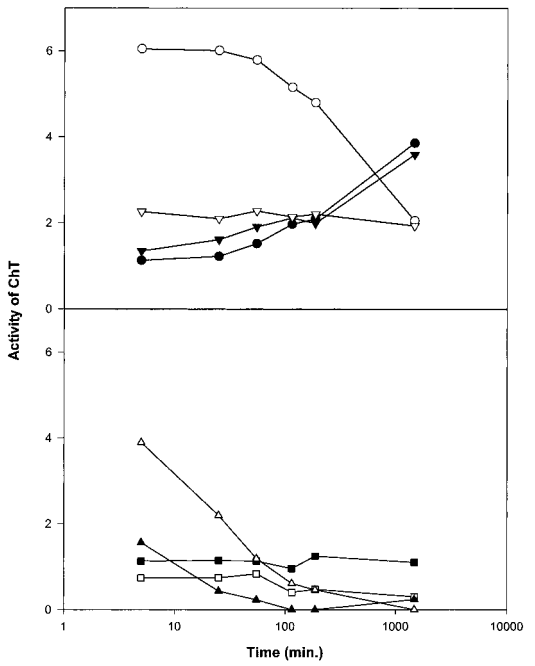


**Fig. 4.** The effect of **1** over time on the different 1:1 ChT–PI complexes. ChT–STI (●), ChT–STI–**1** (○), ChT–BBI (▼), ChT–BBI–**1** (▽), ChT–OMTK (▲), ChT–OMTK–**1** (△), ChT–BPTI (■), and ChT–BBI–**1** (□). Chromogenic substrate used for detecting ChT activity was BTNA (140 $\mu$M) and concentration of ChT, PIs, and **1** for kinetic studies were fixed as 350 nM, 350 nM, and 1.1 $\mu$M, respectively in 5 mM phosphate (pH 7.4) and 30 mM NaCl.

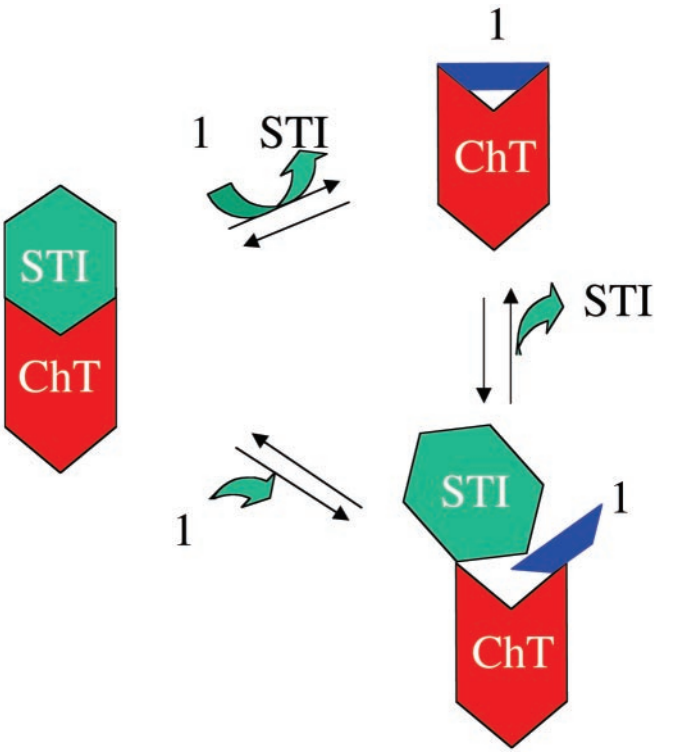


**Fig. 5.** Possible mechanisms for the interaction of **1** with ChT–PI complexes.

M (25). In contrast, the complexes of ChT with BBI, BPTI, and OMTK show $K_d$ values of $5.3 \times 10^{-8}$ (26), $1.0 \times 10^{-8}$ (27), and $5.5 \times 10^{-12}$ M (28), respectively. A critical component of the interaction in all cases is a peptide loop that projects from the surface of the PI and makes contact with active site residues in ChT. As a result, the ChT–PI affinity does not directly correlate with surface area of contact. However, the active site binding loop from the PI is susceptible to cleavage by ChT, leading to hydrolytic modulation of PI activity.

Comparison of the time-dependent inhibition results for ChT (Fig. 4) points to a particularly effective disruption of the ChT–STI complex by **1**. There are lesser effects on ChT complexes with OMTK and BBI and almost no effect on the ChT–BPTI interaction. Further details of the mechanism by which **1** caused an initial recovery of enzymatic activity with the ChT–STI complex come from nondenaturing gel electrophoresis and gel filtration chromatography. These both point to the rapid formation of an initial ternary complex followed by a slower expulsion of the PI and imposition of the inhibitory property of **1**. The sensitivity of the ChT–STI complex to disruption by synthetic receptor **1** is almost certainly caused by its relatively high $K_d$ value. In comparison, receptor **1** has $K_i$ and $K_i$* values in the $10^{-6}$ to $10^{-7}$ M range, making a competitive displacement of the ChT–STI complex reasonable under the conditions of the experiment. The higher affinities of the ChT–BBI, -OMTK, and -BPTI complexes represent a significant thermodynamic barrier to disruption and sizeable effects are only seen (with BBI and OMTK) at higher concentrations of **1** (Fig. 6).

However, the relative binding affinities of the ChT–PI complexes are unlikely to be the only factors in determining the properties of **1**. The formation of a ternary complex in which the PI is still bound and, at least initially, enzyme activity is recovered points to a role for the flexibility of the PI in its sensitivity to disruption by **1**. The formation of a ternary complex in the case of STI presumably requires contact of both the PI and **1** with closely positioned positively charged domains on the surface of ChT. This arrangement would require a conformational accommodation by STI to permit binding of **1** to a region close to the active site. This effect, in turn, accounts for the initial recovery in ChT catalytic activity caused by disruption of the PI–ChT active site interactions. STI is a relatively flexible protein containing two disulfide bonds within its 198 residues and readily undergoes thermal denaturation in aqueous solution (29). In contrast, BPTI is a smaller, more rigid protein with three disulfides that significantly retains its structure even after cleavage of the active site binding loop (30). BBI contains seven disulfide bonds within 78 aa and as a result is stable even in 90% ethanol solution. Several of the smaller PIs have been shown to be stable to denaturation by 8 M urea solution at room temper-

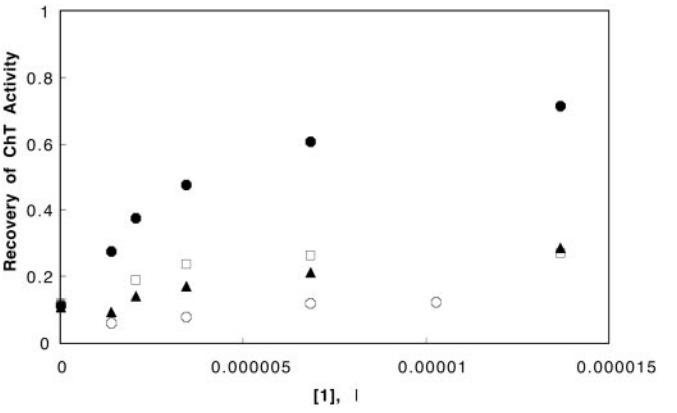


**Fig. 6.** Initial recovery of inhibited ChT activity. After 5 min incubation of ChT (350 nM) with 1.0 $\mu$M of STI (●), OMTK (□), BBI (▲), and BPTI (○), ChT activities were checked as varying concentration of **1** up to 14 $\mu$M. By curve fitting, $K_d$ value of **1** for ChT was obtained as 18 nM.

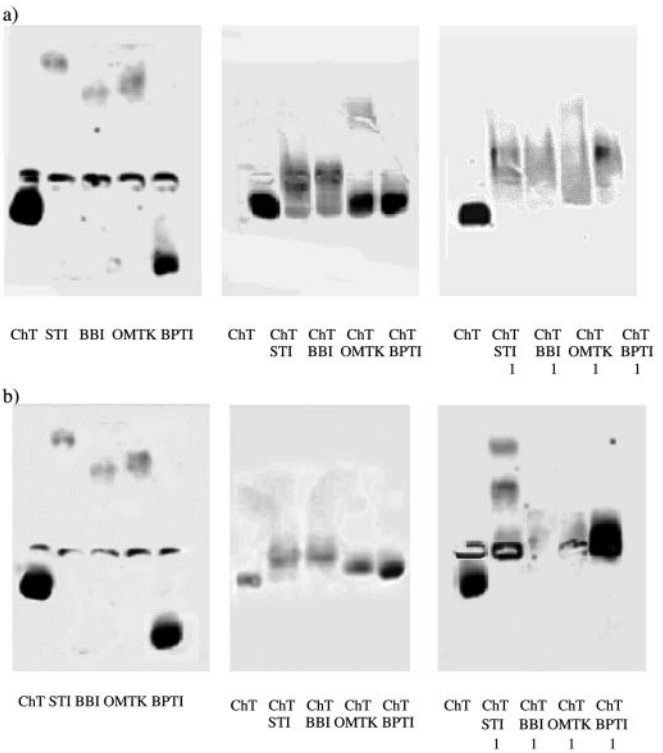


**Fig. 7.** Gel-shift assay (*a*) 10 min incubation and (*b*) 24 h incubation. One percent agarose, 5 mM Na-phosphate gel buffer (pH 7.4) was used for gel preparation and concentration of each component was fixed as [ChT] = 15 $\mu$M, [PIs] = 16 $\mu$M, and [**1**] = 34 $\mu$M.

ature. In the case of the more rigid PIs a conformational change is less accessible and the access of the small substrate into the ternary complex appears to be disfavored. The time-dependent expulsion of STI from the surface of ChT presumably follows the slow binding kinetics of **1** and the conformational change that is necessary for it to achieve optimal interaction with ChT.

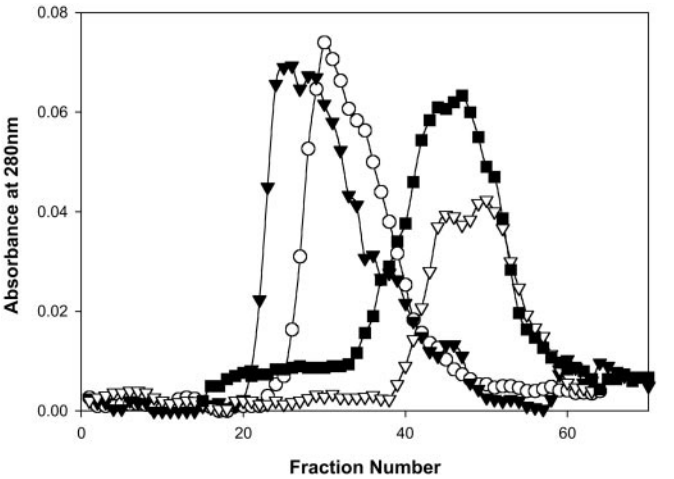


**Fig. 8.** Detection of formation and time-dependent disruption of ternary complex by using size-exclusion column. (▽) ChT alone, (○) after 10 min incubation with ChT and STI, (▼) after 10 min incubation with ChT, STI, and **1**, and (■) after 36 h incubation with ChT, STI, and **1** in 5 mM phosphate buffer, pH 7.4. [ChT] = 20 $\mu$M, [STI] = 20 $\mu$M, and [**1**] = 35 $\mu$M.

In summary, we have discovered that a synthetic molecule designed to contain a large and functionalized surface area is able to bind to the exterior surface of ChT and block the protein–protein interaction with a PI. In the case of the ChT–STI complex this disruption is highly effective and involves the initial formation of a ternary ChT–STI–**1** complex followed by a slow expulsion of the PI. The final ChT–**1** complex also showed much reduced enzyme activity, confirming that the overall process involves replacement of one inhibitor (PI) by another (**1**). However, the initial recovery of enzyme activity suggests that an intermediate state exists where **1** functions as a disruptor of the ChT–PI interaction and not as an inhibitor.

We thank the National Institutes of Health (Grant GM 35208) for financial support of this work.

1. Hartwell, L. H., Szankasi, P., Robert, C. J., Murray, A. W. & Friend, S. H. (1997) *Science*, **278**, 1064–1068.
2. Tilley, J. W., Chen, L., Fry, D. C., Emerson, S. D., Powers, G. D., Biondi, D., Varnell, T., Trilles, R., Guthrie, R., Mennona, F., *et al*. (1997) *J. Am. Chem. Soc.* **119,** 7589–7590.
3. Huang, Z., Li, S., Gao, J., Satoh, T., Friedman, T. M., Edling, A. E., Koch, U., Choksi, S., Han, X. & Korngold, R. (1997) *Proc. Natl. Acad. Sci. USA* **94,** 73–78.
4. Degterev, A., Lugovskoy, A., Cardone, M., Mulley, B., Wagner, G., Mitchison, T. & Yuan, J. (2001) *Nat. Cell Biol.* **3,** 173–182.
5. Wang, J. L., Liu, D., Zhang, Z. J., Shan, S., Han, X., Srinivasa, S. M., Croce, C. M., Alnemri, E. S. & Huang, Z. (2000) *Proc. Natl. Acad. Sci. USA* **97,** 7124–7129.
6. Tzung, S.-P., Kim, K. M., Basanez, G., Giedt, C. D., Simon, J., Zimmeberg, J., Zhang, K. Y. J. & Hockenbery, D. M. (2001) *Nat. Cell Biol.* **3,** 183–191.
7. Peczuh, M. W. & Hamilton, A. D. (2000) *Chem. Rev.* **100,** 2479–2494.
8. Hamuro, Y., Calama, M. C., Park, H. S. & Hamilton, A. D. (1997) *Angew. Chem. Int. Ed. Engl.* **36,** 2680–2683.
9. Kawashima, S. (1997) in *Biomedical and Health Research*, eds. Hopsu-Havu, V. K., Jarvinen, M. & Kirschke, H. (IOS Press, Amsterdam), Vol. 13, pp. 447–452.
10. Powers, J. C. & Harper, J. W. (1986) in *Research Monographs in Cell and Tissue Physiology*, eds. Barrett, A. J. & Salvesan, G. (Elsevier, Amsterdam), Vol. 12, pp. 55–152.
11. Stein, P. E. & Carrell, R. W. (1995) *Nat. Struct. Biol.* **2,** 96–113.
12. Whisstock, J., Skinner, R. & Lesk, A. (1998) *Trends Biochem. Sci.* **23,** 63–67.
13. Moir, R. D., Lynch, T., Bush, A. I., Whyte, S., Henry, A., Portbury, S., Multhaup, G., Small, D. H., Tanzi, R. E., Beyreuther, K. & Masters, C. L. (1998) *J. Biol. Chem.* **273,** 5013–5019.
14. Caswell, M. D., Mok, S. S., Henry, A., Cappai, R., Klug, G., Beyreuther, K., Masters, C. L. & Small, D. H. (1999) *Eur. J. Biochem*. **266,** 509–516.
15. Abts, H. F., Welss, T., Mirmohammadsadegh, A., Kohrer, K., Micel, G. & Ruzicka, T. (1999) *J. Mol. Biol.* **293,** 29–39.
16. Suminami, Y., Nagashima, S., Vujanovic, N. L., Hirabayashi, K., Kato, H. & Whiteside, T. L. (2000) *Br. J. Cancer* **82,** 981–989.
17. Zang, X. & Maizels, R. M. (2001) *Trends Biol. Sci.* **26,** 191–197.
18. Salier, J.-P. (1990) *Trends Biol. Sci.* **15,** 435–439.
19. Bogan, A. A. & Thorn, K. S. (1998) *J. Mol. Biol.* **280,** 1–9.
20. Cochran, A. G. (2000) *Chem. Biol.* **7,** R85–R94.
21. Park, H. S., Lin, Q. & Hamilton, A. D. (1999) *J. Am. Chem. Soc.* **121,** 8–13.
22. Morris, G. M., Goodsell, D. S., Halliday, R. S., Huey, R., Hart, W. E., Belew, R. K. & Olson, A. J. (1998) *J. Comput. Chem.* **19,** 1639–1662.
23. Morris, G. M., Goodsell, D. S., Huey, R. & Olson, A. J. (1996) *J. Comput.-Aided Mol. Des.* **10,** 293–304.
24. Goodsell, D. S. & Olson, A. J. (1990) *Proteins Struct. Funct. Genet.* **8,** 195–202.
25. Bidlingmeyer, U. D. V., Leary, T. R. & Laskowsky, M., Jr. (1972) *Biochemistry* **11,** 3303–3309.
26. Turner, R., Liener, I. E. & Lovrien, R. E. (1975) *Biochemistry* **14,** 275–282.
27. Capasso, C., Rizzi, C., Menegatti, E., Ascenzi, P. & Bolognesi, M. (1987) *J. Mol. Recogn.* **10,** 26–35.
28. Fujinaga, M., Sielecki, A. R., Read, R. J., Ardelt, W., Laskowski, M., Jr. & James, M. N. G. (1987) *J. Mol. Biol.* **195,** 397–418.
29. Bode, W. & Huber, R. (1992) *Eur. J. Biochem.* **204,** 433–451.
30. Laskowski, M., Jr. & Sealock, R. W. (1971) in *The Enzymes*, ed. Boyer, P. D. (Academic, New York), Vol. III, pp. 375–473.